REVIEW OF EXPERIMENTAL RESULTS ON PHOTON-PHOTON INTERACTIONS

Rudolf J. Wedemeyer

Physikalisches Institut der Universität Bonn

Bonn, Federal Republic of Germany

For many years the annihilation process $e^+e^- \longrightarrow \gamma^* \longrightarrow X$

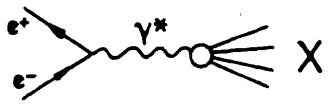

has been the main objective of the experimental activities at e^+e^- colliders. But with the higher beam energies now available also the supplementary two-photon process $e^+e^- \longrightarrow e^+e^-\gamma\gamma \longrightarrow e^+e^-X$

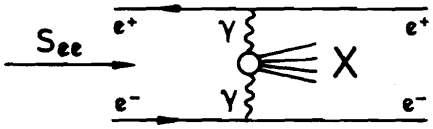

has attracted more and more attention.

The ultimate goal of such experiments is the investigation of the process $\gamma\gamma \longrightarrow X$.

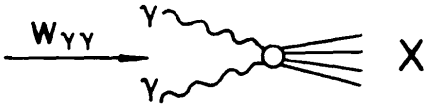

Two photons collide and produce a final state X, which can be a lepton or a hadron pair, a resonance or a multi-hadronic system. In principle all combinations of quasi-real, virtual or highly virtual photons can occur in the initial state.
The angular distribution of the final state electrons (e^+ or e^-) is enormously peaked at small angles with respect to the e^+e^- beams. The energies transferred to the photons are distributed like $1/E_\gamma$.
Thus the colliding photons move predominantly parallel to the beams, and in almost all collisions the incoming photons have significantly different energies.

Consequently the system X exhibits the following characteristics:
- The CMS energy of the $\gamma\gamma$ system, $W_{\gamma\gamma}$, is considerably lower than the energy of the e^+e^-system: $\sqrt{S_{ee}} = 2 \cdot E_{beam}$
- The system X is Lorentz-boosted almost in beam direction.

These characteristics can be used to identify two-photon events without the detection of either one of the scattered electrons. In this 'no tag' case almost all colliding photons are quasi-real. In a typical storage ring detector, as sketched in Fig. 1, the system X is measured in the central detector.
A second possibility to identify two-photon events is the detection of at least one of the scattered electrons in one of the tagging devices (Fig.1). This 'single tag' requirement reduces the rate significantly. Even for the small angle tagger the reduction factor is $\lesssim 1/10$.

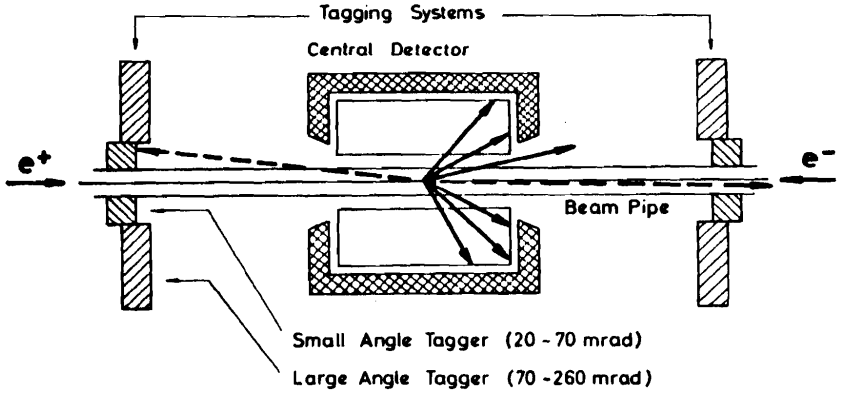

Fig.1 Simplified sketch of a two-photon event in a typical storage ring detector

Tagging, however, furnishes additional information. The kinematical parameters of the tagged photon, in particular its mass (Q^2), can be determined.

Since the way a photon interacts depends on Q^2 special aspects of two-photon physics can be selected by choosing the tagging conditions.

This review is restricted to hadronic final states. It covers the following topics:

I EXCLUSIVE HADRONIC CHANNELS
- Resonances
- Exclusive cross sections near threshold

II INCLUSIVE HADRON PRODUCTION
- High-p_T hadrons
- Photon structure functions

The experiments have been performed at the storage rings SPEAR, DCI and PETRA.

I EXCLUSIVE HADRONIC CHANNELS

The accessible range of the invariant mass, M_X, of exclusively measured hadronic states (or equivalently, of the CMS energy, $W_{\gamma\gamma}$, of the two-photon system) is limited by experimental conditions.

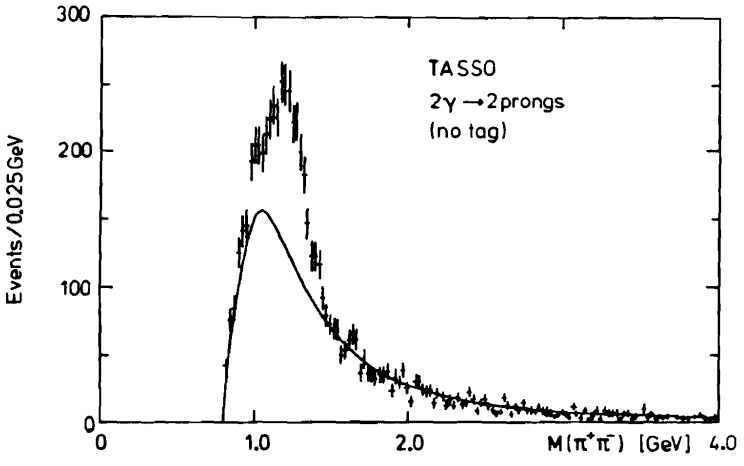

Fig.2 Invariant mass distribution of exclusive two-prong events measured in the TASSO detector. The solid curve is the calculated contribution of lepton pairs.

As an example Fig.2 shows the M_X distribution of $\gamma\gamma$ induced two-prong events recorded in the TASSO detector. Pion masses were assigned to all particles. The number of events corresponds roughly to the first two years of PETRA operation at e^+e^- energies $\sqrt{s_{ee}}$ between 27.4 and 36.7 GeV.
The hadronic signal appears superimposed on a large background of electron and muon pairs (solid curve). Without positive particle identification this background has to be calculated and subtracted. The general shape of the distribution exhibits two distinct features. It falls rapidly towards higher masses ($\sim 1/M_X^3$) mainly due to the decreasing photon fluxes. The cut-off at low masses reflects the trigger conditions and acceptance cuts of the individual experiment.
Thus, even if particle identification is possible the accessible M_X range is limited at lower masses by the necessary experimental cuts and at higher masses by poor statistics ($M_X \lesssim 2$ GeV for the time being).

Resonances

The production of exclusive hadronic states in $\gamma\gamma$ collisions is a unique place to study resonances with C = + and J = 0,2,... New resonances may be found and experimentally unknown properties of known resonances, such as the radiative width $\Gamma_{\gamma\gamma}$, can be determined.

The experimental results reviewed in this paper have been obtained by MARK II at SPEAR, CRYSTAL BALL, CELLO, PLUTO and TASSO. The results are all based on 'no tag' data.
No new resonance has been observed. But there are good and consistent results on the radiative widths of the known resonances

$$\begin{array}{lll} \eta'(958) & J^{PC} = 0^{-+} \\ f^0(1270) & J^{PC} = 2^{++} \\ A_2(1310) & J^{PC} = 2^{++}. \end{array}$$

For the ε (~1200) $J^{PC} = 0^{++}$ an upper limit $\Gamma_{\gamma\gamma}(\varepsilon) \cdot B(\varepsilon \to \pi^+\pi^-) < 1.5$ keV (95% c.l.) has been derived by the TASSO collaboration[1].

The measurements of the radiative width of the f° shall be discussed first since this is a good example to demonstrate what has been achieved in two-photon physics.

$\Gamma_{\gamma\gamma}(f^0)$

Fig.3 shows the preliminary mass distribution of exclusive two-prong events (histogram with error bars) obtained by CELLO[2]. The invariant masses were calculated assuming zero masses for all particles. It should be emphasized that in this experiment the experimental cut-off is comparatively low. The histogram without error bars represents the calculated contribution of lepton pairs.

For a preliminary analysis the calculated background of lepton pairs was normalized and subtracted yielding the signal presented in Fig.4. It shows an enhancement in the mass region of the f° but it also shows a non-f° contribution, which is visible at lower masses, but may well extend to masses larger than the f° mass.
Taking only those events which are in the nominal f° mass region (shaded area) CELLO derived a preliminary result for the radiative width of

$$\Gamma_{\gamma\gamma}(f^0) = 3.6 \pm 0.2 \pm 0.7 \text{ keV}$$
(stat. and syst. error, resp.)

A detailed analysis of the $\pi^+\pi^-$ mass region between 0.6 and 2.0 GeV is in progress.
Already the preliminary signal (Fig.4) demonstrates that for a full analysis of the $\pi^+\pi^-$ channel in this mass range also a non-f° contribution has to be explained. Different approaches have been discussed by MARK II[3] and TASSO[1] (see below).

The pure f° signal is described by a relativistic Breit-Wigner ansatz

$$\sim \frac{\Gamma_{\gamma\gamma}\cdot\Gamma_{\pi\pi}}{(W_{\gamma\gamma}^2 - M_f^2)^2 + M_f^2\Gamma^2}\cdot\sum a_j\left|Y_j^{\lambda}(\cos\Theta^*)\right|^2 \qquad (1)$$

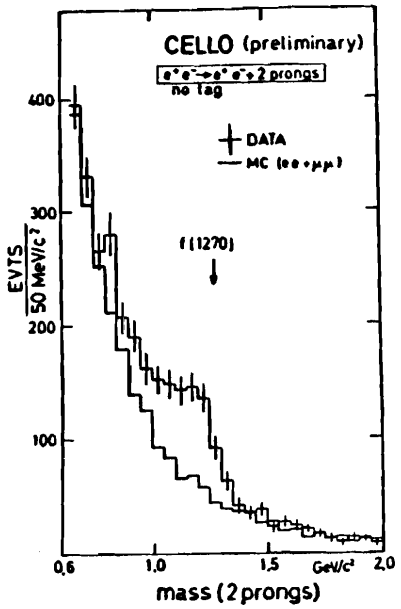

Fig.3 Invariant mass distribution of exclusive two-prong events measured by CELLO. The histogram without error bars is the calculated contribution of lepton pairs.

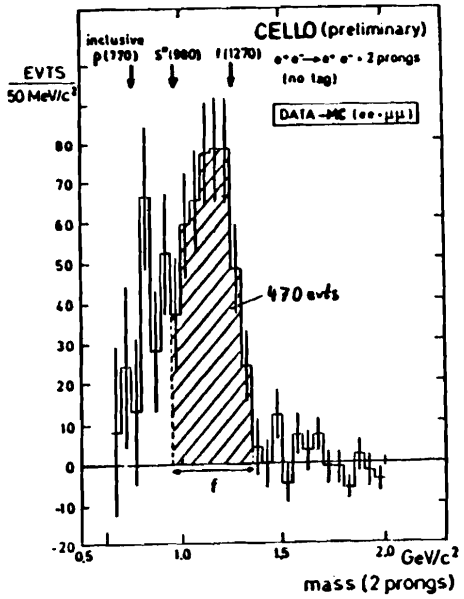

Fig.4 Preliminary f° signal in the $\pi^+\pi^-$ channel obtained by CELLO after background subtraction

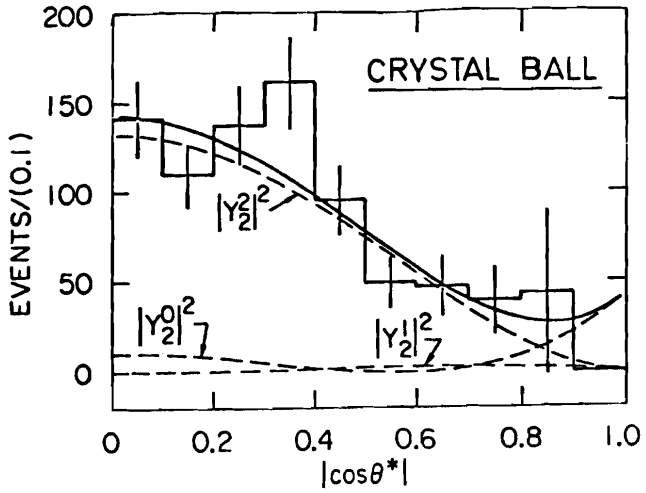

Fig.5 Acceptance corrected decay angular distribution of $f^0 \to \pi^0\pi^0$ observed in the CRYSTAL BALL. The curves are fit results (see text).

In order to determine the parameters J and λ TASSO and CRYSTAL BALL[4] have studied the measured decay angular distributions. Their data clearly favor J = 2 over J = 0 thus giving further support to the assumption that the considered object is the f°.
Only the CRYSTAL BALL experiment has an angular acceptance large enough to perform a complete helicity analysis. This group fitted the angular part of formula (1) with J = 2 to the measured data. The result is presented in Fig.5 (solid curve) in comparison with the data (histogram). The three contributions (λ = 0,1,2) to the fit are separately shown as broken lines. This analysis reveals the dominance of the helicity state λ = 2 in accordance with the theoretical expectation for the production of a J = 2 resonance by two quasi-real photons[5].

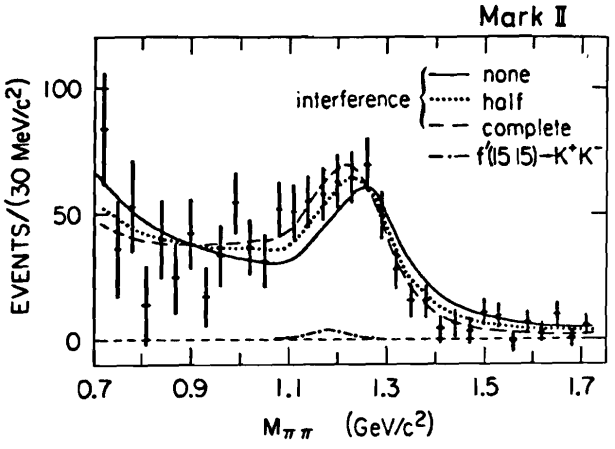

Fig.6 f° signal in the $\pi^+\pi^-$ channel obtained by MARK II. The curves are fit results explained in the text.

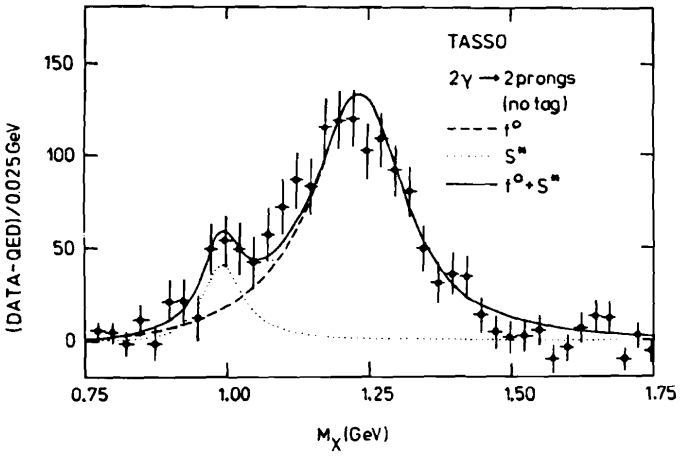

Fig.7 f° signal in the $\pi^+\pi^-$ channel obtained by TASSO. The curves are fit results explained in the text.

For the evaluation of $\Gamma_{\gamma\gamma}$(f°) the CRYSTAL BALL group used the experimentally determined mixture of helicity states while the other experiments assumed a pure λ = 2 state.
As mentioned above, the non-f° contribution to the $\pi^+\pi^-$ signal has been studied by MARK II and TASSO.
The MARK II group has investigated the possibility of a $\pi^+\pi^-$ continuum, interfering with the Breit-Wigner amplitude of the f°. Fit results of this type are compared with the measured $\pi^+\pi^-$ signal in Fig.6. The three upper curves were obtained calculating the continuum from a simple Born term ansatz and varying the degree of interference. In addition, a possible contribution from the process $\gamma\gamma \rightarrow f' \rightarrow K^+K^-$ (where the kaons are mislabled as pions) was calculated and turned out to be small (3.8% of the f° signal, dashed dotted line).
The TASSO group has also studied possible explanations for the non-f° background such as a $\pi^+\pi^-$ continuum and contributions from the resonances f' and ε. Their $\pi^+\pi^-$ signal is shown in Fig.7. It contains the largest number of events (1490). The shape of the distribution looks somewhat different from the one observed by MARK II (Fig.6). The data show a small enhancement near 1 GeV. However, it should be stressed that in the mass region below about 1 GeV the acceptance of the experiment decreases rapidly (comp.Fig.2) and the systematic uncertainties become large.

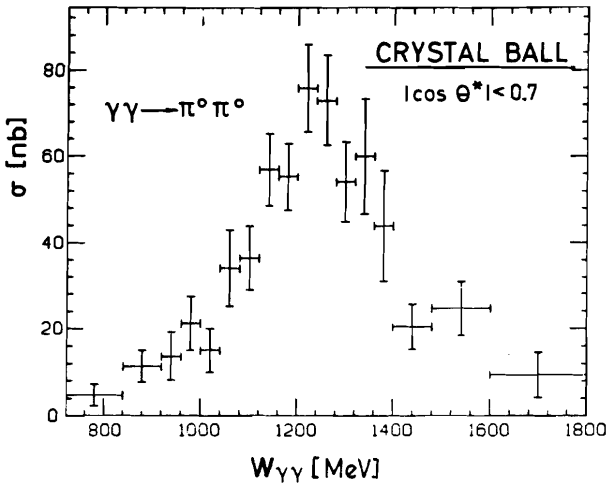

Fig.8 f° signal in the $\pi^\circ\pi^\circ$ channel observed in the CRYSTAL BALL

The TASSO group obtained a good fit to the data describing the signal by the sum of two non-interfering Breit-Wigner functions with standard values[6] for the masses and the widths of the f° and the S* resonances. The solid curve in Fig.7 represents the fit result while the dashed and the dotted lines show the contributions of the two resonances separately.
For the time being the nature of the non-f° part of the signal is an open question. More accurate data, in particular from experiments with good acceptance for masses below 1 GeV, are needed. In addition an improved theoretical treatment of the $\pi^+\pi^-$ continuum has to be developed (see discussion in refs. 1 and 3).

Fortunately the investigations done by MARK II and TASSO have shown that the value of $\Gamma_{\gamma\gamma}(f^\circ)$ does not critically depend upon the particular choice of the model for the non-f° background. Nevertheless, this uncertainty adds to the systematic error.

No such non-f° problem has turned up in the CRYSTAL BALL experiment which has measured the totally neutral channel $f^\circ \to \pi^\circ\pi^\circ$. The most recent result of this group[7] is the f° signal shown in Fig.8. It is the only result presented in absolute terms, giving a peak cross section of about 75 nb. The shape of the signal was found to be entirely compatible with a Breit-Wigner description of the f° resonance assuming a mass of 1233 MeV, which is about 3% lower[8] than the standard value[6], and the standard width. Although there is no significant sign of a non-f° contribution in the data a small background may still be present. In this experiment the mass region below about 1 GeV is affected by the acceptance. Depending on running conditions the energy threshold was set between 600 and 1200 MeV.
In order to facilitate a comparison the experimental results on the radiative width of the f° are summarized in Table 1.

All five results agree well within the errors. The average is close to $\Gamma_{\gamma\gamma}(f^\circ) = 3$ keV.
The statistical errors show that a level of a few percent may well be reached. In the case of the TASSO and the CELLO experiment it is already down to 6%.

Collab.	Chann.	$\Gamma_{\gamma\gamma}(f^\circ)$ ± stat. ± syst. error	Ref.
PLUTO	$\pi^+\pi^-$	2.3 ± 0.5 ± 0.35 keV	9
MARK II	$\pi^+\pi^-$	3.6 ± 0.3 ± 0.5 keV	3
TASSO	$\pi^+\pi^-$	3.2 ± 0.2 ± 0.6 keV	1
CELLO	$\pi^+\pi^-$	3.6 ± 0.2 ± 0.7 keV	2
		(preliminary)	
CRYST.B.	$\pi^\circ\pi^\circ \to 4\gamma$	$2.9 \,^{+\,0.55}_{-\,0.39}$ ± 0.6 keV	4

Table 1: Experimental results on the radiative width of the f° resonance

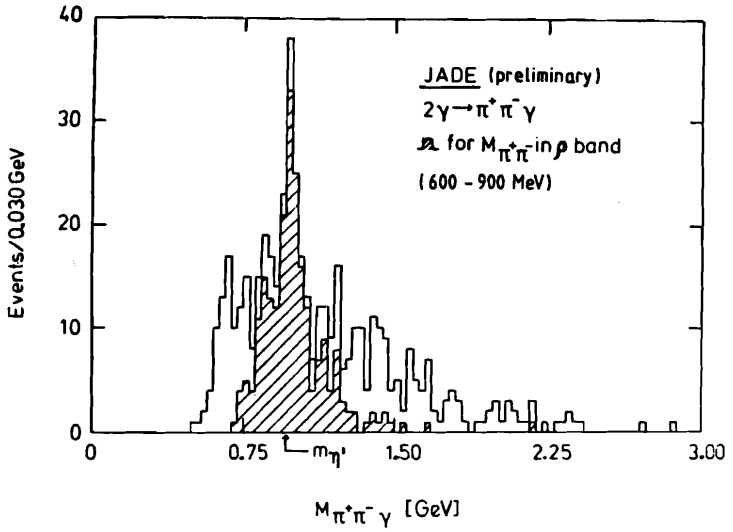

Fig.9 Preliminary η' signal in the $\varrho^0\gamma$ channel obtained by JADE

The systematic errors, however, are still comparatively large (15-20%). They reflect the experimental difficulties discussed above. Among the numerous theoretical predictions for $\Gamma_{\gamma\gamma}(f^0)$, ranging from 1 to 20 keV, two are very close to the average experimental result. One calculation[10] is based on the non-relativistic quark model. It predicts $\Gamma_{\gamma\gamma}(f^0)$ = 2.6 keV. The other one[11] starts from finite energy sum rules for $\gamma\pi \rightarrow \gamma\pi$. With improved experimental input this calculation gives $\Gamma_{\gamma\gamma}(f^0)$ = 3.0 keV.

$\Gamma_{\gamma\gamma}(\eta')$

There is a well known result on the radiative width of the scalar meson η'. It was published by the MARK II group already in 1979[12]. In the meantime also the JADE collaboration has investigated the channel $\eta' \rightarrow \varrho^0\gamma \rightarrow \pi^+\pi^-\gamma$[13]. As shown in Fig. 9 they see a clear signal of about 200 events. The overall histogram is the mass distribution of all $(\pi^+\pi^-\gamma)$ events while the shaded histogram represents the subsample for which the $\pi^+\pi^-$ mass is in the ϱ^0 band ($600 < M(\pi^+\pi^-) < 900$ MeV).

From this subsample JADE derives a preliminary value for the radiative width of the η' which is compared with the MARK II result in Table 2.

Collab.	Chann.	$\Gamma_{\gamma\gamma}(\eta')$ ± stat. ± syst. error	Ref.
MARK II	$\varrho^0\gamma \rightarrow \pi^+\pi^-\gamma$	5.9 ± 1.6 ± 1.2 keV	12
JADE	$\varrho^0\gamma \rightarrow \pi^+\pi^-\gamma$	7.5 ± 0.7 keV (preliminary)	13

Table 2: Experimental results on the radiative width of the η' resonance

Both results agree within the statistical errors. The systematic error of the JADE result is estimated to still be large (50%?).
The quark model for fractionally charged quarks (including phase space corrections) predicts the ratio $\Gamma_{\gamma\gamma}(\eta')/\Gamma_{\gamma\gamma}(\pi^0)$ = 790/1. Taking $\Gamma_{\gamma\gamma}(\pi^0)$ from ref.6 one finds $\Gamma_{\gamma\gamma}(\eta')$ = 6.3 keV which agrees well with the measured values.

$\Gamma_{\gamma\gamma}(A_2)$

A value for the radiative width of the tensor meson A_2 has been reported by two experimental groups. The CRYSTAL BALL collaboration[4] used the channel $A_2 \to \eta\pi^0 \to 4\gamma$ while the JADE group[13] has investigated the channel $A_2 \to \varrho^\pm\pi^\mp \to \pi^+\pi^-\gamma\gamma$.
Fig.10 shows the mass distribution of $\eta\pi^0$ events. This distribution which peaks at the A_2 mass is interpreted as a signal of 25 events over a background of 5-6 events.
The A_2 signal seen by the JADE group is shown in Fig.11. The overall histogram is the mass distribution of all $(\pi^+\pi^-\pi^0)$ events and the shaded histogram represents the subsample of events with the $\pi^+\pi^0$ or the $\pi^-\pi^0$ mass in the ϱ band ($600 < M(\pi^\pm\pi^0) < 1000$ MeV).
The number of events in both experiments is far too small for a study of the decay angular distribution. So both groups determined the radiative width assuming a pure helicity $\lambda = 2$ state for the A_2. The results are compared in Table 3.

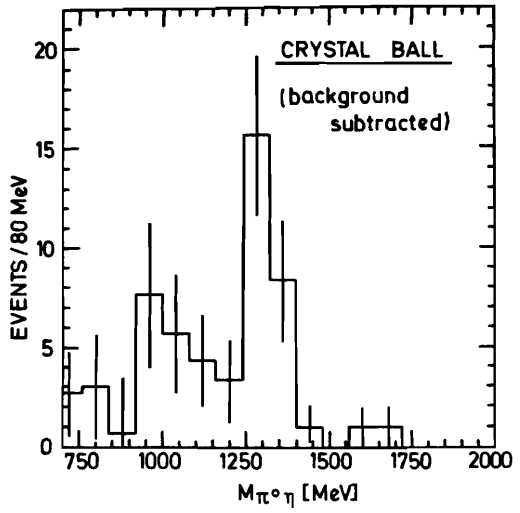

Fig.10 A_2 signal in the $\pi^0\eta$ channel observed in the CRYSTAL BALL

There is agreement within the statistical errors. Again the systematic error of the JADE result is estimated to be large (50%?).
Also these results can be compared to the quark model prediction.
From $\Gamma_{\gamma\gamma}(A_2)/\Gamma_{\gamma\gamma}(f^0) = 9/25$ and taking the above mentioned average value $\Gamma_{\gamma\gamma}(f^0) \approx 3$ keV one expects a $\Gamma_{\gamma\gamma}(A_2) \approx 1$ keV. This is very close to the mean value of the two experimental results.

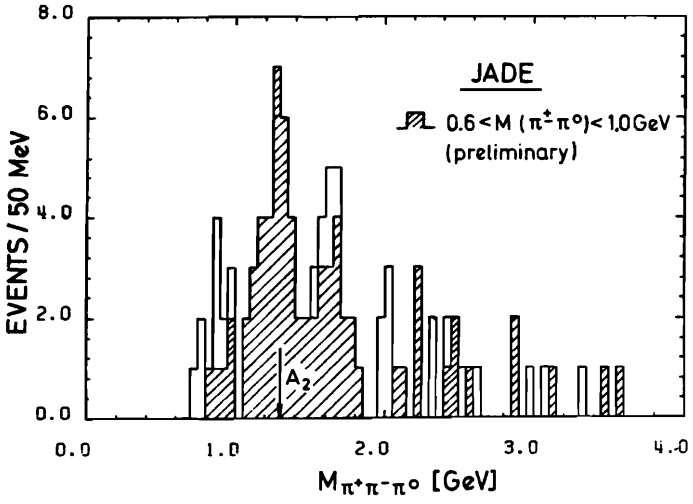

Fig.11 Preliminary A_2 signal in the $\varrho^\pm\pi^\mp$ channel obtained by JADE

Collab.	Chann.	$\Gamma_{\gamma\gamma}(A_2)$ ± stat. ± syst. errors	Ref.
CRYST.B.	$\eta\pi^0 \rightarrow 4\gamma$	0.77 ± 0.18 ± 0.27 keV	4
JADE	$\delta^\pm\pi^\mp \rightarrow \pi^+\pi^-\gamma\gamma$	1.2 ± 0.4 keV (preliminary)	13

Table 3: Experimental results on the radiative width of the A_2 resonance

Exclusive cross sections near threshold

$\gamma\gamma \rightarrow \pi^+\pi^-$

Two-photon induced pion pair production near threshold has been studied at DCI using the detector DM1 and a specific "zero degree" tagging system (Θ_{tag} < 10 mrad)[14].
For all exclusive two-prong events the particle masses were determined from the measured kinematical data. The subsample of e^+e^- pairs was used for normalization and the number of detected $\mu^+\mu^-$ pairs was found to be in good agreement with the QED expectation.
Fig. 12 presents the yield of $\pi^+\pi^-$ pairs as a function of the CMS energy of the two-photon system. The contribution of lepton pairs leaking into this data sample is indicated by the shaded area. The remaining 34 $\pi^+\pi^-$ pairs correspond to a cross section (averaged over $0.3 < W_{\gamma\gamma} < 0.8$ GeV) of (69±15)pb which is larger by 2.5 standard deviations than the expectation from a simple Born ansatz for pion pair production (see also curve in Fig. 12).
A model for two-photon induced pion pair production in this energy range[15] - which is based on a unitarized Born ansatz and which, in addition, assumes a two-photon excitation of a broad scalar object ε (856) - has been fitted to the data (histogram in Fig. 12) yielding a coupling constant of $f^2_{\varepsilon\gamma\gamma}$ = (0.75±0.30)GeV².

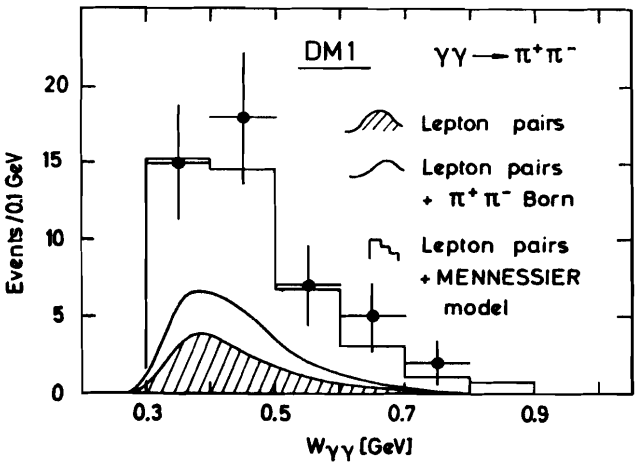

Fig.12 Invariant mass distribution of exclusive $\pi^+\pi^-$ events measured in the detector DM1. The curves show the contribution of lepton pairs and the expectation from a simple Born ansatz for pion pair production. The histogram represents the fit of model[15] to the data.

$\gamma\gamma \to \pi^+\pi^-\pi^+\pi^-$

The TASSO collaboration has been the first to study the two-photon production of the exclusive 4π state. 'No tag' data with an average Q^2 of 0.05 GeV^2 were used covering an energy range of $1.5 < W_{\gamma\gamma} < 2.1$ GeV. Early results based on 89 events were published in 1980 [16]. They have shown that at energies near threshold

a) the reaction $\gamma\gamma \to \pi^+\pi^-\pi^+\pi^-$ proceeds predominantly through the channel $\gamma\gamma \to \rho^0\rho^0$ and

b) the cross section for the reaction $\gamma\gamma \to \rho^0\rho^0$ (77 ± 12 nb at maximum) is much larger than the VDM estimate.

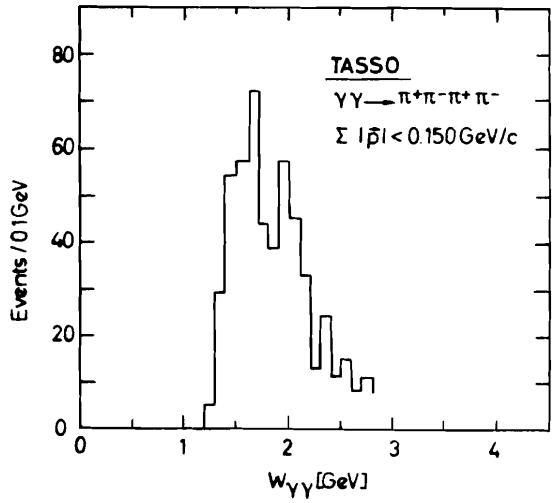

Fig.13 Invariant mass distribution of exclusive $\pi^+\pi^-\pi^+\pi^-$ events measured by TASSO

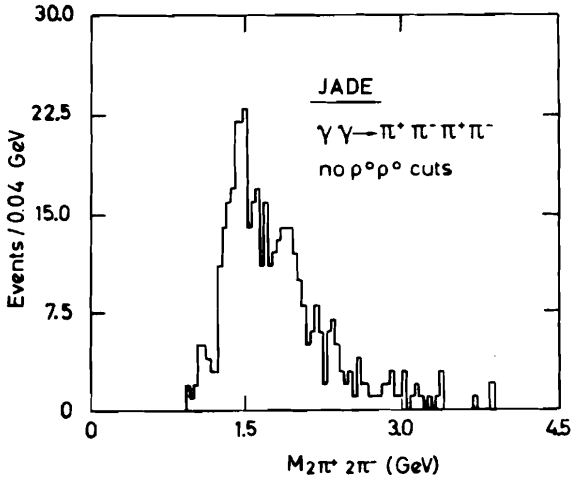

Fig.14 Invariant mass distribution of exclusive $\pi^+\pi^-\pi^+\pi^-$ events measured by JADE

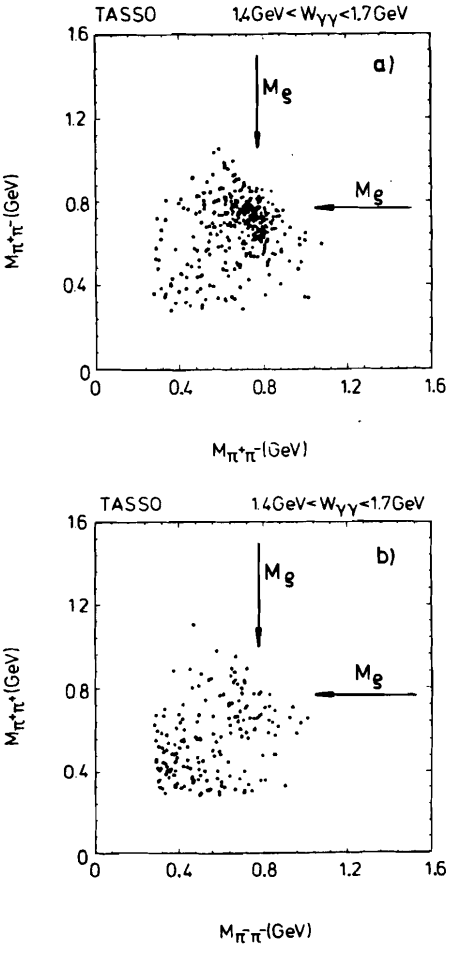

Fig.15 Two-dimensional distribution of pion pair masses, a) for neutral and b) for charged pair combinations in inclusive $\pi^+\pi^-\pi^+\pi^-$ events measured by TASSO

These general features have been confirmed by results from MARK II at SPEAR[17] and by preliminary data from JADE[13] and CELLO[2].
In the meantime the statistical accuracy of the TASSO data has improved significantly. A total number of 533 exclusive 4π events is now available. Their energy distribution (not corrected for efficiency) is shown in Fig.13. It can be compared with the corresponding data obtained by the JADE collaboration (Fig.14) which exhibits the same features. There is a steep rise from the threshold region to 1.5 GeV (about $2 \cdot M_{\varrho}$). It is much steeper than the energy dependence of the experimental acceptance in this energy range. The maximum is followed by a shoulder at about 1.7 GeV and a decrease towards higher energies.
The evidence for the dominance of the channel $\gamma\gamma \rightarrow \varrho^0\varrho^0$ as observed by TASSO is presented in Figs.15a and b. Fig.15a shows the two-dimensional mass distribution for neutral pion pairs ($\pi^+\pi^-$). Because of the two possible combinations of such pairs there are two entries per event. In spite of the combinatorial background one can clearly see the high population density in the area where both pairs have masses close to the ϱ^0 mass. The corresponding plot for charged pion pairs (Fig.15b, one entry per event) does not exhibit any $\varrho^0\varrho^0$ signal.
Since the statistical accuracy is improving with time and in view of the possibility of a structure in the four-pion yield (Figs.13 and 14) a refined analysis is necessary. Possible contributions other than $\gamma\gamma \rightarrow \varrho^0\varrho^0$ (e.g., $\varrho^0\pi^+\pi^-$, $\pi^+\pi^-\pi^+\pi^-$ uncorrel.) have to be investigated and isolated. The angular distributions for the different channels have to be studied carefully. The latter is most important for the calculation of the different efficiencies which have to be known for a determination of the cross sections.
Up to now the experimental groups have used different approaches to extract acceptance corrected angular distributions from their data. The results look different (comp., e.g., refs.2 and 17). However, these differences are statistically marginal.
The TASSO group has started a new and more complex analysis which is still in progress. New cross section data from TASSO are not yet available due to the above mentioned difficulties. No cross sections have been reported by JADE so far.

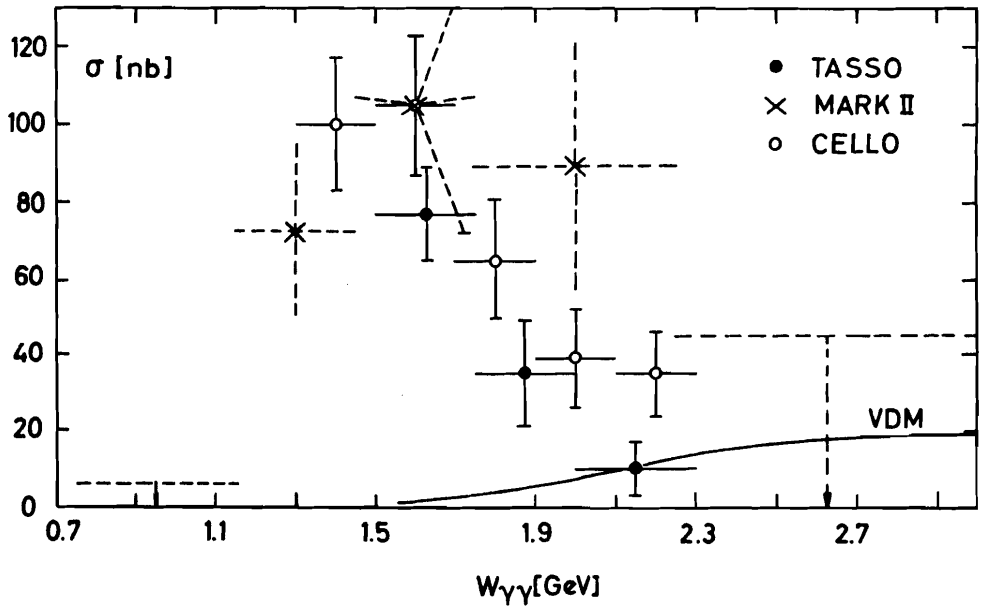

Fig.16 Comparison of cross section data from TASSO (1980, $\gamma\gamma \rightarrow \varrho^0\varrho^0$), MARK II ($\gamma\gamma \rightarrow \pi^+\pi^-\pi^+\pi^-$) and CELLO ($\gamma\gamma \rightarrow \pi^+\pi^-\pi^+\pi^-$, but with $M(\pi^+\pi^-)$ in the ϱ^0 band). The curve represents the VDM expectation.

The MARK II and the CELLO group have derived cross sections using simplifying assumptions which they found to be consistent with their data.
The MARK II cross sections were calculated from all four-pion events. For the determination of the detector acceptance this group used a Monte Carlo simulation of the reaction $\gamma\gamma \to \rho^0\rho^0$ assuming distributions for the production and the decay angle which are consistent with the experimentally determined angular distributions. The CELLO group adopted the same procedure for the acceptance calculation. But they took only those events where both pion pairs have masses in the region of the ρ^0 mass ($0.6 < M(\pi^+\pi^-) < 0.9$ GeV).
The cross sections of both experiments are compared with the early TASSO results for $\gamma\gamma \to \rho^0\rho^0$ in Fig.16. Taking into consideration that the three sets of data are the results of different approaches the agreement is reasonable. In addition, the new data from MARK II and CELLO give information on the behavior of the cross section below 1.5 GeV. The curve in Fig.16 represents the VDM expectation for the channel $\gamma\gamma \to \rho^0\rho^0$, extrapolated down to the production threshold. It can by no means explain the measured cross section.
The early TASSO results have stimulated a number of theorists to study possible explanations for the surprisingly large $\rho^0\rho^0$ or $\pi^+\pi^-\pi^+\pi^-$ cross section. Various and different attempts have been reported[18]. They are certainly a valuable input to future discussions. But for the time being no conclusions can be drawn. The $\gamma\gamma$ production of exclusive four-pion states has turned out to be rather complex and challenging. More detailed information has to be and will be furnished by the experiments.

$\gamma\gamma \to p\bar{p}$

The most recent investigation of an exclusive channel has been reported by the TASSO collaboration[19]. Baryon pair production in two-photon collisions has been observed for the first time.
The 'no tag' two-prong sample was examined for a contribution from the channel $\gamma\gamma \to p\bar{p}$.
Particles were identified by determining their masses from the momentum and an absolute time-of-flight measurement. Fig.17 shows the two-dimensional mass plot. There are 8 events, well separated from the rest, for which the masses of the positive and the negative particle are both close to the proton mass. These 8 events correspond to an integrated luminosity of 19000 nb^{-1} and yield a cross section (averaged over $2.0 < W_{\gamma\gamma} < 2.6$ GeV) of

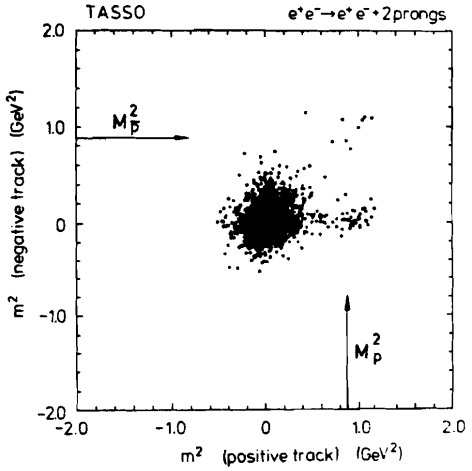

Fig.17 Two-dimensional distribution of particle masses in exclusive two-prong events measured by TASSO

$$\sigma(\gamma\gamma \to p\bar{p}) = 4.5 \pm 1.6 \pm 0.8 \text{ nb}.$$

In the framework of VDM this process is related to the inverse processes $p\bar{p} \to \rho\rho$ and $p\bar{p} \to \rho\omega$. An estimate based on data for the latter two reactions gives a cross section which is only 20% of the measured one.

II INCLUSIVE HADRON PRODUCTION

High-p_T hadrons

The production of multi-hadronic states in two-photon collisions can proceed via two different mechanisms. The photon reacts like a hadron or it couples directly to quarks in a point-like manner as described in lowest order by the graph:

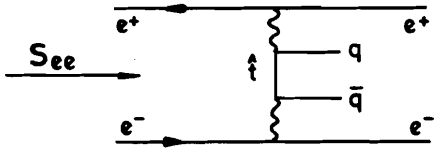

Experimental results which give evidence for this 'point-like' contribution to the multi-hadronic cross section have been reported by PLUTO, TASSO and JADE.

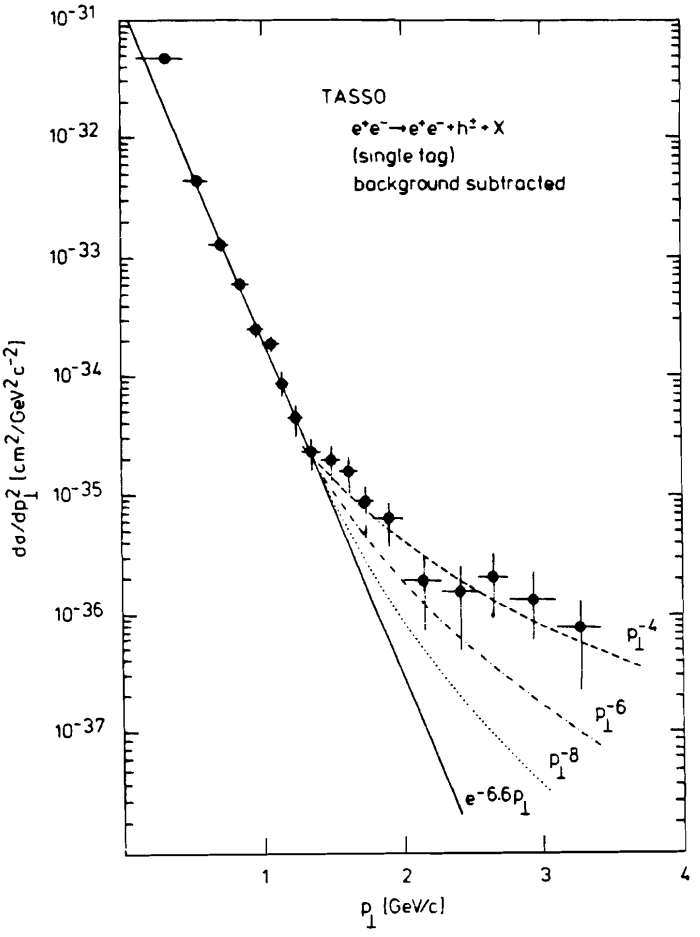

Fig.18 Distribution of transverse hadron momenta in multi-hadronic events measured by TASSO. For comparison different functional forms for the p_T dependence are shown.

One way to look for the 'point-like' contribution is to study the inclusive cross section $d\sigma/dp_T^2$ as a function of p_T, where p_T is the transverse momentum of a produced hadron with respect to the direction of motion of the two-photon system (practically the e^+e^- beam axis). From dimensional counting the 'point-like' production mechanism is expected to give rise to a p_T^{-4} behavior of the p_T distribution. This may be observed at high p_T where the steeply falling 'hadronic' contribution has become comparatively small.

As an example Fig.18 presents the inclusive p_T distribution for charged hadrons measured by TASSO[20]. 'Single tag' data are used in order to keep the contamination by misidentified events from 1γ-annihilation as low as possible.
The average Q^2 is 0.35 GeV² and the average $W_{\gamma\gamma}$ is about 6 GeV. The distribution exhibits a steep exponential fall-off at low p_T and a long tail towards high p_T. It has been analyzed by fitting the function

$$d\sigma/dp_T^2 = c_1 \cdot \exp(a \cdot p_T) + c_2 \cdot (p_T)^b \qquad (2)$$

to the data yielding b = -3.9 ± 0.6 for the exponent, in good agreement with the expectation.

This evidence for the 'point-like' contribution is a most interesting result. It has been obtained for fairly low values of p_T and at energies $W_{\gamma\gamma} \leq 10$ GeV whereas in hadron-hadron collisions ($pp \rightarrow \pi + X$) the inclusive p_T distribution has been found to approach the expected p_T^{-8} behavior only for much higher energies.

If the high-p_T hadrons are produced via the point-like coupling of the photons to quark lines (graph at the beginning of this chapter) hard scattering should lead to the production of two-jet events:

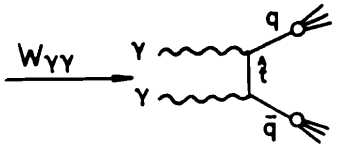

In this case the momentum transfer $|\hat{t}|$ (proportional to p_T^2 of the quarks) is large and the transverse momenta of the jets, p_T(jet), are expected to be high.

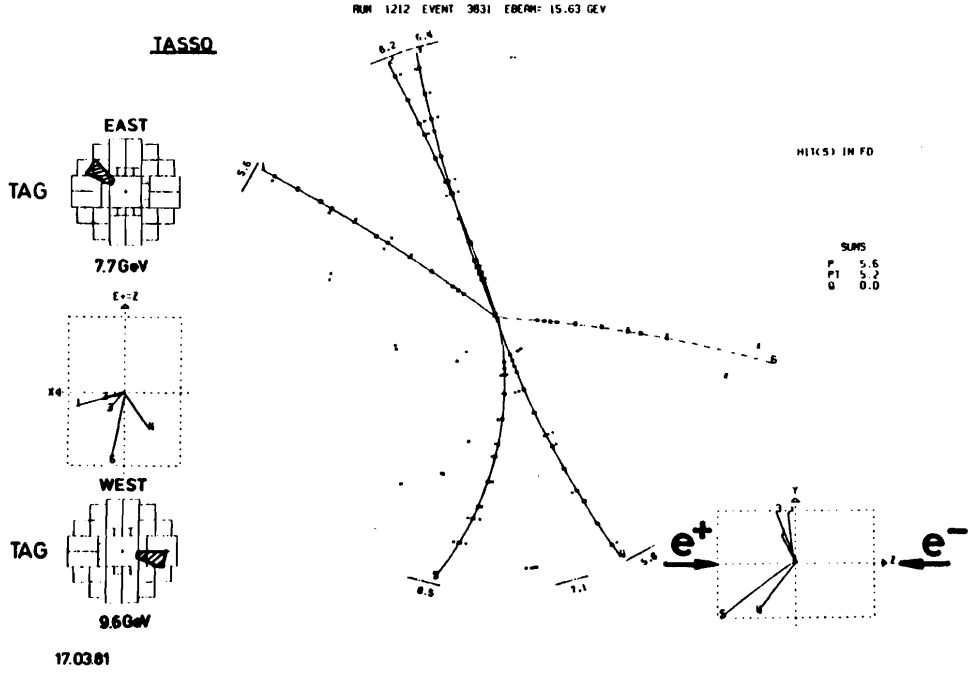

Fig.19 A two-jet candidate event recorded in the TASSO detector

The basic formula

$$d\sigma/d\hat{t}(\gamma\gamma \rightarrow 2 \text{ jets}) = 3 \cdot \sum_{N_f} e_q^4 \cdot d\sigma/d\hat{t}(\gamma\gamma \rightarrow \mu^+\mu^-) \qquad (3)$$

relates the 'jet cross section' to the prototype of a point-like process, muon pair production.
An experimental determination of the ratio $R_{\gamma\gamma} = 3 \cdot \sum e_q^4$ which depends on the fourth power is probably the most sensitive test for the quark charges. For fractionally charged u, d, s, c quarks it is expected to be 34/27.

From equation (3) it can readily be shown that $d\sigma/dp_T^2(\text{jet}) \sim p_T^{-4}(\text{jet})$ and the experimental groups have tried to detect this power law.

That there are two-jet events among the large number of multi-hadronic events may - in some cases - be seen by eye. Fig.19 gives an example. The event viewed along the e^+e^- beam line (central part of the figure) exhibits two jets. They are boosted in beam direction as shown in the inserts. The left hand part of the figure demonstrates that this is one of the rare 'double tag' events.

The experimental groups PLUTO[21], TASSO[20] and JADE[22] have selected two-jet candidate events from the sample of multi-hadronic events employing procedures

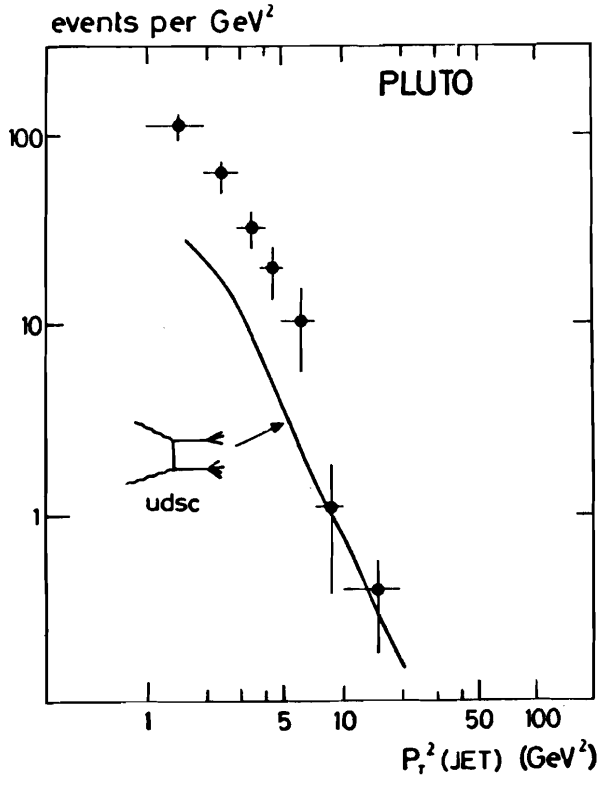

Fig.20 Distribution of transverse jet momenta observed by PLUTO. The curve represents the absolute prediction for $\gamma\gamma \rightarrow q\bar{q}$ with fractionally charged quarks u,d,s,c.

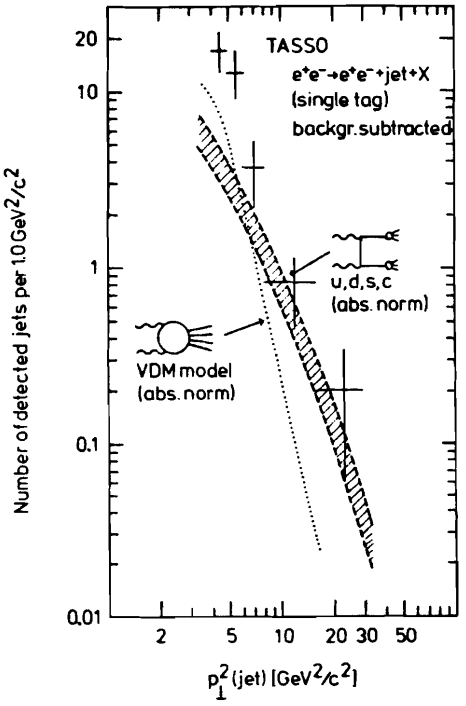

Fig.21 Distribution of transverse jet momenta observed by TASSO. The dotted line shows the absolute VDM expectation and the shaded band represents the absolute prediction for $\gamma\gamma \rightarrow q\bar{q}$ using four different fragmentation models.

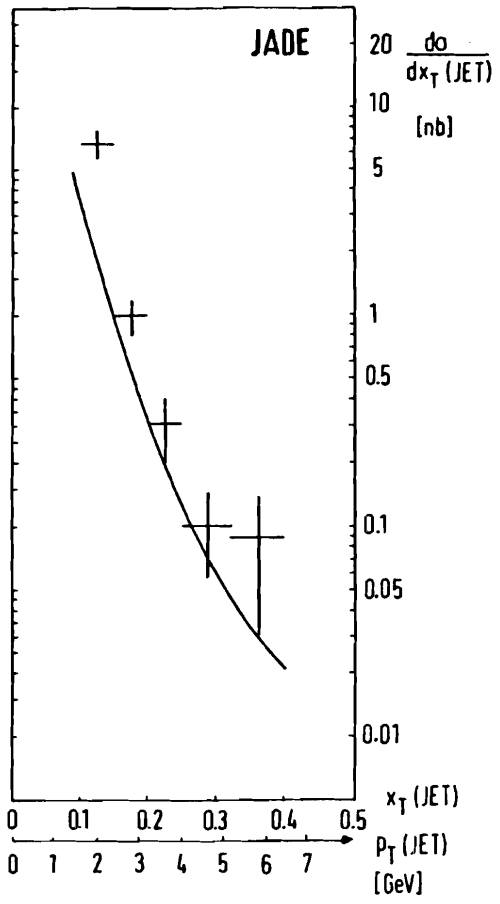

Fig.22 Distribution of transverse jet momenta observed by JADE. The curve represents the absolute prediction for $\gamma\gamma \to q\bar{q}$ with fractionally charged quarks u,d,s,c.

similar to the ones which have been used to study jet production in 1γ-annihilation. These procedures have been modified for the search for two non-collinear jets. About 40 two-jet candidate events have been found by each of the three groups. The p_T^2(jet) distribution measured by PLUTO is shown in Fig.20. The data are compared with an absolute calculation according to equation (3) and taking $R_{\gamma\gamma} = 34/27$. Fig.21 shows the corresponding result from TASSO. Here the absolute prediction based on equation (3) appears as a shaded band rather than a curve. It demonstrates the effect of different models (Field-Feynman model, all pion model with longitudinal phase space) and varied parameters for the fragmentation part of the calculation. For comparison the expectation from a VDM model is also shown (dotted curve). It does not explain the data in this p_T range.
The JADE group have used the variable $x_T = p_T(\text{jet})/E_{beam} = 2p_T(\text{jet})/\sqrt{S_{ee}}$ instead of p_T. They present the x_T distribution in Fig.22. The curve, again, is the prediction of the hard scattering model (eqn.(3)) with $R_{\gamma\gamma} = 34/27$.

In all three experiments the data are above the expectation for two-jet production via $\gamma\gamma \to q\bar{q}$ but they appear to approach it with increasing p_T.
This is an intriguing result and the experimental groups try hard to improve and complement it. They have to cope with a number of difficulties.
In general, judging from the experience with jets in 1γ-annihilation the energies $W_{\gamma\gamma} \lesssim 10$ GeV are marginal for jet studies. On the experimental side the determination of p_T(jet) is difficult since, due to the Lorentz boost of the $\gamma\gamma$ system, fragments at small polar angles escape detection. Moreover, the background from 1γ-annihilation leads to a substantial correction, particularly at high p_T(jet).

Another difficulty arises from the fact that the reaction $\gamma\gamma \to q\bar{q}$ is not the only source of high-p_T jets.

QCD predicts reactions like, e.g., $\gamma\gamma \to q\bar{q}g$.

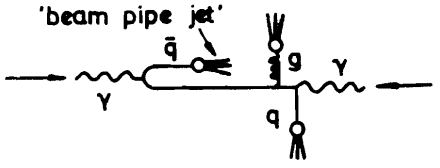

The hard scattering occurs between one photon and a quark from the other photon producing two high-p_T jets. The remaining quark fragments into a third jet in the extreme forward direction. $d\sigma/dp_T^2$(jet) is proportional to p_T^{-4}(jet) (as for the reaction $\gamma\gamma \to q\bar{q}$). The cross section is expected to be smaller than that for $\gamma\gamma \to q\bar{q}$ but only by less than an order of magnitude[23].

Another source of high-p_T jets are higher twist reactions, e.g., $\gamma\gamma \rightarrow q\bar{q}$ + meson

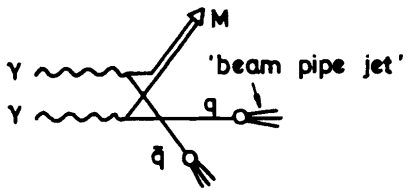

Again the hard scattering produces two high-p_T jets and a third one developes in the extreme forward direction. In this case $d\sigma/dp_T^2(jet)$ is proportional to $p_T^{-6}(jet)$ but the cross section is expected to be smaller than that for $\gamma\gamma \rightarrow q\bar{q}$ only if $p_T(jet) > 4$ GeV/c [23].

In principle these competing processes could be identified by detecting hadrons at very small polar angles. However, none of the detectors which have been used for the above investigations was designed for that purpose.

Photon structure functions

Under certain kinematic conditions the investigation of multi-hadron production via the two-photon mechanism

$$e^+e^- \rightarrow e^+e^-\gamma\gamma \rightarrow e^+e^- + \text{multi-hadr.} \qquad (4)$$

offers the possibility to extract information on the structure functions of the photon.
If one of the photons is highly virtual ($Q^2 > 1$ GeV^2) and the other one is quasi-real ($k^2 \approx 0$) process (4) can be described as deep inelastic electron-photon scattering in complete analogy to deep inelastic electron-nucleon scattering. The electron scatters off a quasi-real 'target' photon exchanging a highly virtual photon

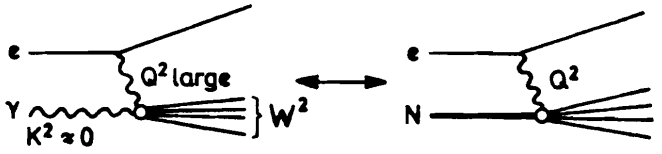

The cross section for the $e\gamma$ scattering can conveniently be expressed in terms of the scaling variables

$$x = \frac{Q^2}{Q^2 + W^2} \quad \text{and} \quad y = 1 - \frac{E-E_\gamma}{E} \cdot \cos^2\Theta/2$$

and the structure functions $F_i(x, Q^2)$.

$$\frac{d\sigma}{dx\,dy}\Big|_{e\gamma \rightarrow eX} = \frac{16\alpha^2 EE_\gamma}{Q^4}\left\{(1-y)F_2 + xy^2F_1\right\} \qquad (5)$$

(E and Θ denote the energy and the scattering angle of the electron, E_γ the energy of the exchanged photon.)

The variables Q^2 and y are completely determined by the kinematic parameters of the scattered electron measured in the tagging device. But there is an experimental problem with the variable x. Not W but $W_{vis} < W$ is measured in the central detector. An unfolding procedure ($x_{vis} \rightarrow x$) is necessary in order to obtain results as a function of x.

Under experimental conditions the angle θ is small (in the PLUTO experiment $\theta_{max} = 15°$). Thus $y \ll 1$ and the cross section (5) can be approximated by

$$d\sigma/dxdy\,\big|_{e\gamma \rightarrow eX} \sim (1/Q^4)(1-y)F_2(x, Q^2) \qquad (6)$$

This approximation has been used to extract information on the structure function F_2 from the data.

Results have been reported by the PLUTO collaboration[24]. In addition to the small angle tagging system (SAT, 20-70 mrad) the PLUTO detector has also a large angle tagger (LAT) covering angles from 70 to 260 mrad.

Events were selected which have
a) a tag in the LAT on one side ($1 < Q^2 < 15$ GeV^2 at $\langle\sqrt{s_{ee}}\rangle = 31$ GeV) and
b) no tag in either the SAT or the LAT ('anti-tagging', $k^2 \approx 0$).

111 events of this type were found.

The unfolding procedure was done with the help of a Monte Carlo simulation of $e\gamma$ scattering in the PLUTO detector. Not knowing the functional form of F_2, events were generated according to formula (6) with a constant F_2. The decay of the hadronic system was described by a limited p_T phase space model.
This simulation was found to reproduce - within the errors - the experimental distributions of Q^2, W_{vis} and x_{vis} well enough to be used for the unfolding correction.

In Fig.23 the measured F_2/α, averaged over the Q^2 range of the experiment, is plotted versus x. Averaging over Q^2 does not introduce a serious problem. It has been shown by a Monte Carlo study (see lower part of Fig.23) that the average Q^2 hardly varies for $0.1 < x < 0.9$. So the data in Fig.23 correspond to an almost constant $Q^2 \approx 5$ GeV^2.

Considering the errors F_2 appears to be more or less flat with an average of about $0.35\,\alpha$.
The results are compared with theoretical expectations[25]. The dotted curve shows an estimate [26] for the 'hadronic' contribution to F_2

$$F_2^{\gamma} \approx \frac{\alpha}{f_\gamma^2/4\pi} \cdot \frac{1}{4}(1-x) \qquad (7)$$

It is certainly too small to be the only contribution. The solid curve describes the sum $F_2^{\gamma} + F_2^{QCD}$, where

$$F_2^{QCD} = h(x)\cdot\ln(Q^2/\Lambda^2) \qquad (8)$$

is the leading order QCD result[27], calculated for u, d, s quarks and with $\Lambda = 0.2$ GeV.

The effect of higher order corrections is demonstrated by the dashed dotted curve which represents the results of ref. 28, also for a Λ of 0.2 GeV. Both expectations are compatible with the data.

The contribution of the c-quark (dashed curve) is small. It was calculated from the bare quark box diagram assuming a mass of 1.5 GeV.

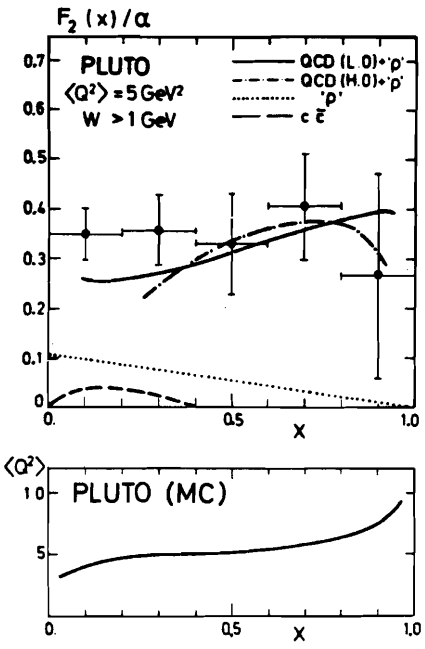

Fig.23 Photon structure function $F_2(x)$ for $Q^2 \approx 5\ GeV^2$ measured by PLUTO. The curves represent theoretical expectations (see text). The lower figure shows the Q^2-x correlation in this experiment (MC study).

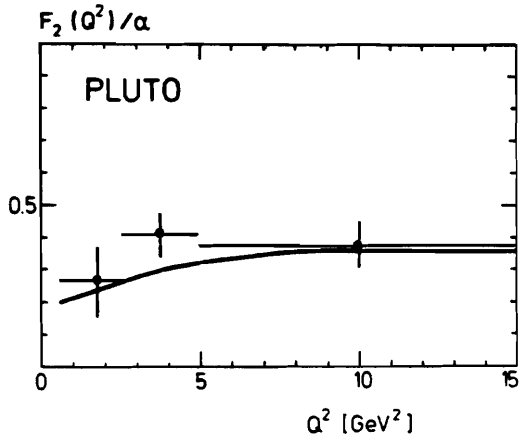

Fig.24 Dependence of F_2 on Q^2, averaged over $0.2 < x_{vis} < 0.8$, measured by PLUTO. The curve represents the leading order QCD prediction.

Since the $\ln Q^2$ dependence of F_2 represents a strong scale breaking the PLUTO group has made an attempt to see this effect in their data. In Fig.24 F_2/α is plotted versus Q^2. In order to avoid strong Q^2-x correlations (see lower part of Fig.23) F_2 is averaged here over $0.2 < x_{vis} < 0.8$. The curve is the result of the leading order QCD calculation. Data and curve are consistent.

Although the errors of the data are too large to draw strong conclusions these are exciting results. This PLUTO experiment has taken a first look at a structure function of the photon.

Summary

The radiative widths of the resonances η', f^0, and A_2 have been determined with good accuracy and the results of different experiments agree well within the errors. The experimental uncertainties are dominated by systematics. In particular, the channel $\gamma\gamma \to \pi^+\pi^-$ shows non-f^0 contributions whose nature is still an open question.
Cross sections near threshold have been measured for two-photon production of the exclusive two-pion and four-pion final states and most recently also the process $\gamma\gamma \to p\bar{p}$ has been observed. For all these channels the measured cross sections near threshold are larger than the VDM estimate. This is particularly true for the four-pion channel which has turned out to be rather complex and challenging. It is clearly dominated by $\varrho^0\varrho^0$ production. But with improved statistics a detailed investigation of all contributions to the four-pion yield has

become necessary, the more, since there is an indication for a structure in the energy dependence of the cross section. Refined analyses are in progress.

Evidence for a direct, point-like coupling of the photons to quark pairs has been observed in multi-hadron production at high transverse momenta of the hadrons. The p_T distribution shows a long tail towards high p_T which is in accordance with the p_T^{-4} power law expected from dimensional counting. It is most interesting that this behavior becomes evident already at energies $W_{\gamma\gamma} \lesssim 10$ GeV.

Intriguing results have been reported on jet production in two-photon collisions. Two-jet candidate events have been observed. With increasing transverse jet momentum the measured distribution of $p_T(\text{jet})$ appears to approach the absolute prediction for two-jet production via $\gamma\gamma \rightarrow q\bar{q}$ with fractionally charged u, d, s, c quarks.

The structure function $F_2(x,Q^2)$ of the photon has been measured for the first time. Although the experimental uncertainties are still large a comparison with theoretical expectations shows that a purely hadronic behavior of the photon does not explain the measured data. The experimental results are consistent with a leading order QCD calculation ($\Lambda = 0.2$ GeV), however, they do not resolve the effects of higher order corrections.

The experiments which have been performed during the last two years have proven that two-photon physics is a fertile and promising field. In the near future the accuracy of the experimental results will certainly improve and new interesting data will become available. But some of the difficulties discussed in the talk point to deficiencies of the detectors which have been used up to now. In particular, we need real forward detectors rather than tagging devices for an effective exploitation of this fertile field.

Acknowledgement

I would like to thank Dr.H.J. Behrend, Prof.Ch. Berger, Dr.J.E. Olsson, Prof.K. Strauch, and Dr.W. Wagner for communicating their latest results to me and I am very grateful to my colleagues of the TASSO collaboration for their support. I am particularly indebted to Prof.E. Hilger and Prof.H. Rollnik for valuable discussions. Last but not least I gratefully acknowledge the help I received from my scientific secretary H. Kück.

References

1) TASSO collaboration, R. Brandelik et al., DESY 81/026 (June 1981), to be published in Z.Physik C

2) CELLO collaboration, contributed paper to the "Int. Conf. on High Energy Physics", Lisbon (1981)

3) MARK II collaboration, A. Roussarie et al., Phys. Lett. 105B (1981)304

4) D.L. Burke, invited talk at the "4th Int. Colloqu. on Photon-Photon Interactions", Paris (April 1981), SLAC-PUB-2745 (May 1981)

5) P. Grassberger and R. Kögerler, Nucl. Phys. B106 (1976)451
P. Schrempp-Otto, F. Schrempp, T.F. Walsh, Phys. Lett. 36B (1971)463

6) Particle Data Group, Rev.Mod.Phys. 52 (1980)

7) K. Strauch, private communication

8) Incidentally also the $\pi^+\pi^-$ data of the other experiments show a similar mass shift of 30 to 40 MeV. Possible explanations have been discussed by the experimental groups. But no consistent picture has evolved yet.

9) PLUTO collaboration, Ch. Berger et al., Phys.Lett. 94B (1980)254

10) V.M. Budnev and A.E. Kaloshin, Phys.Lett. 86B(1979)351

11) B. Schrempp-Otto, F. Schrempp and T.F. Walsh, Phys.Lett. 36B (1971)463

12) MARK II collaboration, G.S. Abrams et al., Phys.Rev.Lett. 43 (1979)477

13) J.E. Olsson, private communication

14) A. Courau et al., Phys.Lett. 96B (1980)402
A. Falvard et al., paper No. 48, submitted to this conference

15) G. Mennessier, paper No. 42, submitted to this conference

16) TASSO collaboration, R. Brandelik et al., Phys.Lett. 97B (1980)448

17) MARK II collaboration, D.L. Burke et al., Phys.Lett. 103B (1981)153

18) H. Goldberg and T. Weiler, Phys.Lett. 102B (1981)63
J. Layssac and F.M. Renard, Montpellier PM/81/5 (May 1981)
K. Biswal and S.P. Misra, paper No. 12, submitted to this conference
C. Ayala, A. Bramon and F. Cornet, paper No. 115, submitted to this conference

19) TASSO collaboration, R. Brandelik et al., DESY 81/058 (September 1981), and paper No. 237, submitted to this conference

20) TASSO collaboration, R. Brandelik et al., DESY 81/053 (August 1981), submitted to Phys.Lett., and paper No. 232, submitted to this conference

21) D. Cords, invited talk given at the "4th Int. Colloqu. on Photon-Photon Interactions", Paris (1981), DESY 81/033 (June 1981)

22) JADE collaboration, W. Bartel et al., DESY 81/048 (August 1981)

23) S.J. Brodsky, T.DeGrand, J. Gunion and J. Weis, Phys.Rev.Lett. 41 (1978)672 and Phys.Rev. D19 (1979)1418

24) PLUTO collaboration, Ch. Berger et al., DESY 81/051 (August 1981), submitted to Phys.Lett.

25) see W.A. Bardeen, invited talk given at this conference

26) C. Peterson, T.F. Walsh and P.M. Zerwas, Nucl.Phys. B174 (1980)424

27) W.R. Frazer and J.F. Gunion, Phys.Rev. D20 (1979)147

28) W.A. Bardeen and A.J. Buras, Phys.Rev. D20 (1979)166
D.W. Duke and J.F. Owens, Phys.Rev. D22 (1980)2280
A.J. Buras and D.W. Duke, unpublished

Discussion

P. Kessler, College de France: As a comment on $\gamma\gamma \to p\bar{p}$ I would like to remark that this reaction has the interesting feature that the inverse experiment $p\bar{p} \to \gamma\gamma$ may be performed (it needs a different machine, different experimentalists, but it should give the same result apart from a kinematic factor). Actually this experiment was performed some 12 years ago by Hartill et al. at Brookhaven. At 2.26 GeV c.m. energy 2 events were found. The authors performed a careful background analysis and found that the background might account only for a fraction of one event. So, if those two events are taken as significant they involve a quite large cross section (of the order of the Born term prediction or so). Thus it is not surprising that a number of events $\gamma\gamma \to p\bar{p}$ have been found.

R. J. Wedemeyer: The measured cross section was also compared to the Born term expectation. It is much smaller (by about a factor of 10) than the Born term taken in the simple way. As far as a comparison with the inverse reaction is concerned I think statistics has to be improved. The reaction $\gamma\gamma \to p\bar{p}$ has been observed for the first time and the statistical error of the cross section is still large.

P. Kessler, College de France: Perhaps it would be interesting to redo also the inverse experiment.

R. J. Wedemeyer: Certainly. A comparison with the inverse reaction would be much better than with the reactions $p\bar{p} \to \rho\rho$, $\rho\omega$ via VDM.

A. Litke, Stanford: This is a comment related to your observation of $\gamma\gamma \to p\bar{p}$. We have observed in our quark detector at PEP a few hundred two-prong events with each particle travelling at low velocity, $\beta \simeq 0.5$. From the range of these particles we conclude they must be heavy, that is, kaons or pions. Our interpretation is that these events are $\gamma\gamma \to K^+K^-$ or pp^- near threshold. Our detector is especially sensitive to this type of event because it has a very low threshold for triggering, about 30 MeV/particle.

R. J. Wedemeyer: I should point to the fact that the resolution shown in the two-dimensional mass plot was not good enough to separate kaons from light particles like pions. The masses were determined from the times-of-flight and the momenta of the particles.